Supplementary Material

Cellular Patterning Alone Using Bioprinting Regenerates Articular Cartilage through Native-Like Cartilagenesis

Experimental Section

1. 3D Bioprinting

1.1. The bioprinter

The details of the direct-volumetric drop-on-demand (DVDOD) 3D bioprinter have been reported previously. [1][2] In our system, the bioink droplet volume is directly regulated by a linear actuator, a departure from the indirect control mechanisms observed in existing systems, such as modulating fluid-valve opening durations or the pressure applied to the bioink. The bioprinter, in essence, comprises a three-axis linear motion gantry outfitted with multiple linear dispensing units. Each unit integrates a syringe that is propelled by a linear actuator. The volume of bioink expelled from each dispensing tip is manipulated volumetrically by this actuator. When bioink is introduced into the air-driven dispensing nozzle, pulsed air is injected, which propels the predetermined bioink volume out. The dispensing units work in coordination to manage both the dispensed droplets' locations on a substrate and the volume of each droplet. The bioprinter is additionally furnished with units to maintain temperature and humidity. In addition, the same volume of droplet can be dispensed via different drive pressure so that the interaction of the dispensed droplet with the existing bionic on the substrate can be controlled for different outcomes.

The open-source GRBL control system, encompassing GRBL firmware, Arduino Boards, and motor controllers, is utilized to oversee the bioprinter's multiple linear actuator motions. This

includes the XYZ gantry and the linear actuators that regulate the advancement of the syringe plungers. The activation of pulsed air is facilitated through the GRBL's built-in on-off control function. Standard GRBL-supported G-Codes and M-Codes are used to control the motion and the toggling on and off of the pulsed air. Codes are transmitted to the bioprinter via GRBL-compatible code senders (https://github.com/grbl/grbl/wiki/Using-Grbl). Lastly, a pressure regulator ensures the control of the pulsed air's pressure.

1.2. Cell culture and hydrogels

All animal procedures were approved by our Institutional Animal Care and Use Committee (IACUC). Whole articular stifle joints of immature calves were obtained from a local abattoir. The surface of each joint was disinfected with povidone-iodine, and the joint was opened using aseptic techniques. Articular cartilage tissues were collected, and superficial layers were removed. The harvested cartilage tissues were sliced into miniature pieces and digested overnight with 0.2% collagenase type II (Worthington) in DMEM-F12 medium (Invitrogen) at 37 °C. The digested tissues were filtered through cell strainers, and chondrocytes were collected and seeded onto 150 mm Petri dishes (Corning) in DMEM-F12 medium with 10% FBS (Corning) and 1% Penicillin/Streptomycin (Corning). When 80–90% confluence was reached, the chondrocytes were trypsinized and passaged for expansion. The same medium was used for all the following chondrocyte-related assays unless otherwise noted.

Human mesenchymal stem cells (hMSCs) were obtained from the Stem Cell Repository at Texas A&M University, and cultured in complete α-Minimum Essential Medium (αMEM, Gibco) supplemented with 15% fetal bovine serum (FBS, Atlanta Biologicals), 1% penicillin/ streptomycin (Gibco) and 2 mM L-glutamine (Gibco) at 37 °C with 5% CO_2. hMSCs were passaged when they reached 80% confluency. Medium was changed 2–3 times per week.

Both chondrocytes and hMSCs were harvested with 0.25% trypsin/EDTA and resuspended in a composite hydrogel containing collagen and fibrin before bioprinting.

1.3. Bioprinting process

1.3.1. General principle of the cellular patterning using bioprinting

A bioink was made by mixing chondrocytes or hMSCs ($6–10\times10^6$ cells ml^{-1}) with collagen type I (2mg l^{-1}, Advanced BioMatrix) and fibrin (2mg ml^{-1}, Sigma) hydrogels. First, using a discrete dispenser, the bioink was dispensed to the surface of a Petri dish to form a droplet. Droplets containing thrombin (1–2 U ml^{-1}) in DMEM-F12 medium without a hydrogel or cells were dispensed to the first droplet by higher pressure through a second dispenser. Higher-pressure-driven droplets without cells served as disrupting forces when they collided with the first droplet. These forces drove homogeneous cells into clusters while all the droplets merged into one larger droplet on the substrate. The thrombin quickly solidified the bioink, and the newly formed cell patterns were fixed in place without generating interfaces between clusters. This bioprinting process was repeated so that an array of micro-constructs was generated.

1.3.2. Optimize the bioprinter control parameters

The volumes of droplets, driving pressures, number of droplets, and droplet-dispensing locations are the four primary parameters controlling the cellular patterns within a micro-construct. Because there are material batch variations and fluctuations in the cell viscosity and concentration et al. among different assay batches, the same bioprinter control parameters can generate different patterns. Therefore, no universal parameters can be used to generate patterned micro-tissues with good repeatability among different batches of assays. However, within an

assay, these parameters are relatively stable. When the same bioprinter control parameters are used, good repeatability can be achieved within an assay.

The combinations of the different volumes of droplets, driving pressures, number of droplets and the location of droplet-dispensing are used as the bioprinter control parameters, and an array of micro-constructs can be bioprinted. The volume of droplets and the driving pressure are correlated with the sizes of cluster areas within a droplet. The number of droplets and the location of droplet-dispensing affect the uniformity of the clusters.

Therefore, a general protocol is to start a trial using a fixed droplet volume. The driving pressure gradually increases until apparent cellular clusters are observed after liquid colliding. This pressure value is set as low-end driving pressure. Then the driving pressure continues to be increased until the spherical shape of the cell-containing droplet is slightly disrupted, and 90% of this value is set as high-end driving pressure. Different levels of driving pressure can be selected between the low and high-end pressure values. The volume of the droplet can also be varied. The number of droplets is usually chosen between efficiency and cluster uniformity–use the least possible number of droplets to generate good uniformity. Each of the four parameters can be set to several different levels or values, and the parameters of their combinations are used to generate the array.

1.3.3 H-MCTs bioprinting

After the optimized PA-MCTs bioprinting parameters were chosen, the equivalent concentrations of cells and hydrogels in the PA-MCTs were calculated and were used to prepare cells containing hydrogels for H-MCTs bioprinting. H-MCTs used for comparing with corresponding PA-MCTs were directly deposited onto the Petri dish in a two-droplets approach: cell-free thrombin solution in the first droplet and a cell-containing droplet in a composite hydrogel containing collagen

type I and fibrin. The lowest possible pressure was used for H-MCT bioprinting-calibrated for each assay batch. The final concentrations of cells and hydrogels were the same in corresponding PA-MCTs and H-MCTs in each assay. The Petri dishes containing arrays of micro-constructs were transferred to an incubator to polymerize the collagen component fully.

2. Analysis of the distribution of the patterned clusters

2.1. Confocal imaging and chondrocyte pattern analysis

To analyze the size of the patterned cell clusters and the distance between the clusters, the same bioprinting protocol described above was used, except the diameter of each PA-MCT was controlled to be larger (2–3 mm) so that more cell clusters were analyzed. After the hydrogel component of the bioink was fully polymerized, samples were rinsed with PBS and stained with Calcein-AM and imaged under a confocal microscope (Eclipse Ti, Nikon). Acquired images were processed and analyzed using ImageJ. [3] Equivalent circle diameters (ECDs) and maximal inscribed circles were calculated to represent the sizes of cell clusters and distances between clusters. Numbers of cell clusters of different sizes were counted, and the clusters were color labeled according to their sizes.

To visualize cell patterns within a bioprinted PA-MCT, PA-MCTs were rinsed and stained with Calcein-AM (Invitrogen). The patterns of cells were imaged by combining fluorescence confocal microscopy and reflection confocal microscopy using a previously reported protocol. [4]

2.2. Pattern Analysis

We used the distributions of ECDs of cell clusters to represent the patterns of cell clusters within a bioprinted micro-construct. First, the ECD distributions were visualized using Empirical

Cumulative Distribution Function (ECDF) plotting, which can also help select different clusters patterns. Kolmogorov-Smirnov distribution analysis was also used to choose unique patterns among the generated patterns.

2.3. Analyze the relationship between gene expression and the cellular cluster patterns

Replicates of each standard pattern were bioprinted using the same corresponding bioprinter control parameters. Only the replicates with the statistically same distribution as the corresponding standard distribution were included for further pattern analysis. Within the same assay, using the same lot of cells and hydrogels and the bioprinting parameters of the 20 unique patterns, 20 groups of PA-MCTs were bioprinted. The PA-MCTs were further cultured for 3weeks before qPCR analysis for gene expression of the cartilagenesis positively related Col-II, Sox-9 and ACAN and negatively related COL-I.

2.4. PCR scoring

The gene expression of the replicates of each gene in each group was averaged. Each gene expression was then normalized to the highest corresponding average value. The PCR score of an individual sample was calculated using the normalized values and the following equation:

PCR score = PCR_COLII + PCR_Sox9 + PCR_ACAN - PCR_COLI

The PCR score of each pattern was the average score of all the replicates. All the 20 patterns were then ranked according to the averaged PCR scores in descending order. Each pattern was then named according to its ranking; for example, the group with the highest PCR score was named PAT1.

2.5. Pattern Scoring

(i) Area score: the summed area of clusters in a specific ECD range (Table S1) over the total cluster area, which reflects the percentage of cells under the influence of the patterns.

(ii) Number score: the summed number of clusters in a specific ECD range (Table S1) over the total cluster numbers, reflecting patterning efficiency.

Pattern score = (Area score + Number score) / 2

Table S1. 66 ECD ranges for the quantification of cluster distributions.

(1) 20-50 μm	(2) 20-60 μm	(3) 20-70 μm	(4) 20-80 μm
(5) 20-90 μm	(6) 20-100 μm	(7) 20-110 μm	(8) 20-120 μm
(9) 20-130 μm	(10) 20-140 μm	(11) 20-150 μm	(12) 30-60 μm
(13) 30-70 μm	(14) 30-80 μm	(15) 30-90 μm	(16) 30-100 μm
(17) 30-110 μm	(18) 30-120 μm	(19) 30-130 μm	(20) 30-140 μm
(21) 30-150 μm	(22) 40-70 μm	(23) 40-80 μm	(24) 40-90 μm
(25) 40-100 μm	(26) 40-110 μm	(27) 40-120 μm	(28) 40-130 μm
(29) 40-140 μm	(30) 40-150 μm	(31) 50-80 μm	(32) 50-90 μm
(33) 50-100 μm	(34) 50-110 μm	(35) 50-120 μm	(36) 50-130 μm
(37) 50-140 μm	(38) 50-150 μm	(39) 60-90 μm	(40) 60-100 μm
(41) 60-110 μm	(42) 60-120 μm	(43) 60-130 μm	(44) 60-140 μm
(45) 60-150 μm	(46) 70-100 μm	(47) 70-110 μm	(48) 70-120 μm
(49) 70-130 μm	(50) 70-140 μm	(51) 70-150 μm	(52) 80-110 μm
(53) 80-120 μm	(54) 80-130 μm	(55) 80-140 μm	(56) 80-150 μm
(57) 90-120 μm	(58) 90-130 μm	(59) 90-140 μm	(60) 90-150 μm
(61) 100-130 μm	(62) 100-140 μm	(63) 100-150 μm	(64) 110-140 μm
(65) 110-150 μm	(66) 120-150 μm		

ECD: equivalent circle diameter

2.6. Select the optimized ECD range using Spearman's Rho correlation analysis

The pattern scores calculated using 66 different ECD ranges were ranked in descending order. Spearman's Rho rank correlation was performed between the pairs of PCR score ranking and each of the 66 pattern score rankings. The ECD range of the pattern score with the highest correlation with

the PCR score will be chosen as the optimized score range to select the optimized chondrogenesis pattern.

3. Micro-tissue culture

After each micro-construct was fully solidified, medium was added to the Petri dishes. PA-MCTs containing chondrocytes were cultured in DMEM/F12 (Gibco) supplemented with 10% FBS. PA-MCTs containing hMSCs were cultured in the following chondrogenic medium: high glucose (4.5 g l^{-1}) Dulbecco's Modified Eagle's Medium (DMEM-HG, Invitrogen), 10% ITS + Premix Tissue Culture Supplement (Becton Dickinson), 10^{-7} M dexamethasone (Sigma), 1 μM ascorbate-2-phosphate (Sigma), 1% sodium pyruvate (Invitrogen) and 10 ng ml^{-1} transforming growth factor-beta 1 (TGF-β1, Stemimmune LLC) up to 3 weeks. All the micro-constructs were cultured at 37 °C with 5% CO_2.

4. Bio-assembly assays

4.1. Single PA-MCT migration assay

Individual PA-MCTs or H-MCTs were cultured for 2 weeks and then aspirated from the Petri dish and transferred to wells of a 96-well plate (one sample per well) and embedded with a mixed hydrogel composed of collagen and fibrin. After the fibrin component was quickly polymerized with thrombin, the 96-well plate was transferred to an incubator for further polymerizing the collagen component. After the hydrogels were fully solidified, 300 μl of culture medium was added to each well. All the samples were cultured at 37 °C with 5% CO_2. After 24 h, the samples were washed with phosphate-buffered saline (PBS), fixed with paraformaldehyde, and stained with Alcian blue. At least triplicate samples were assayed.

4.2. PA-MCTs and H-MCTs bio-assembly assay with less than 20 MCTs

PA-MCTs or H-MCTs were cultured for 2 weeks and then collected and transferred into the wells (< 20 MCTs/well) of a round-bottom 96-well plate so that they attached to each other within a well, and covered with a composite hydrogel composed of collagen and fibrin. After the hydrogel was quickly polymerized with thrombin, the plate was transferred to an incubator for further polymerizing the collagen component. After the hydrogel in each well was fully solidified, each sample was transferred to a well of a 24 well plate. Two ml of culture medium was added to each well, and the samples were cultured at 37 °C with 5% CO_2 for 5 weeks. The assembly dynamic was tracked daily under an inverted microscope (Nikon), and at least triplicate samples were terminated each week for histological analysis.

4.3. PA-MCTs and H-MCTs bio-assemble into large macro-cartilage

PA-MCTs and H-MCTs were collected after 2 weeks of culture. PA-MCTs or H-MCTs were added to transwells (~500/well) and covered with a mixed hydrogel composed of collagen and fibrin. The hydrogel was quickly polymerized with thrombin and transferred to an incubator for further polymerization. After the hydrogel was fully solidified, the medium was added to the well to cover both under and above the constructs. Two ml of culture medium was added to the well and the samples were cultured at 37 °C with 5% CO_2 for 5 extra weeks. The medium was changed twice per week. At least triplicate samples were assayed for each condition and each group.

4.4. Bio-assembly tracking using live imaging

PA-MCTs bioprinted using hMSCs were placed in a glass-bottom Petri dish and covered with a mixed hydrogel composed of collagen and fibrin. The hydrogel was quickly polymerized with thrombin and transferred to an incubator for further polymerization. After the hydrogel was fully solidified, medium (detailed in 3) was added to the well. The dynamic of the bio-assembly process of PA-MCTs was tracked and recorded using an inverted microscope at 37 °C with 5% CO_2.

5. Integration assays

5.1. Harvesting and decellularizing articular cartilage, bone and osteochondral tissues

Cartilage, bone and osteochondral tissues were removed from bovine diarthrodial joints and processed into cylindrical and cuboid tissues using stainless steel punches and an oscillating saw. The cuboid bone tissues were flushed with pressured water to remove bone marrow and other debris. The tissues were placed in a jar filled with a 1% sodium dodecyl sulfate solution and were processed on an orbital shaker to remove cells. Sheep stifle joints were obtained locally and also from sacrificed sheep in other research studies as approved by our IACUC. The stifle joints were used for modeling PA-MCT delivery and repairing large cartilage defects. For the latter, intact individual condyles were removed from stifle joints and decellularized using the same protocol described above. The intact distal ends of the femurs of mature rabbits were removed using an oscillating saw, and all tissues superficial to the bone were removed with a scalpel and decellularized using the same protocol described above.

After the decellularization process, all the tissues were rinsed with distilled water and PBS sequentially and were sterilized with 70% ethanol before use.

5.2. Integration assay on cylindrical cartilage and bone tissues

An agarose solution was cast into wells of 12-well plates and solidified. Holes were punched in the agarose gels to match the sizes of cylindrical cartilage or bone tissues generated previously. PA-MCTs and H-MCTs were cultured for 2 weeks and then collected from the Petri dish. PA-MCTs or H-MCTs were placed on top of the cylindrical tissues and covered with a mixed hydrogel composed of collagen and fibrin. The hydrogel was quickly polymerized with thrombin, and the plates were transferred to an incubator for further polymerizing the collagen component. After the hydrogel was fully solidified, medium was added to the wells and samples were cultured at 37 °C with 5% CO_2. After 1–2 days of culture, constructs including the bone or cartilage tissues and the added PA-MCTs or H-MCTs were removed from the agarose wells and transferred to wells of 6-well plates and cultured for 5 extra weeks. The medium was changed twice a week, and at least triplicate samples were assayed for each condition and group.

6. Repairing cartilage defects in an osteochondral explant model

6.1. Surface contour fitting assay

As shown in Figure S15 (Supporting Information), silicone sheets with convex or concave edge surfaces were placed between two glass slides and held vertically. PA-MCTs were gently placed over the surfaces. To evaluate if the PA-MCTs could self-fit to the curvature of the surfaces, images were taken using a stereo-microscope which was perpendicularly orientated to the glass slides and evaluated by two independent scientists.

6.2. Medium size defect repair

As shown in Figure S1 (Supporting Information), cuboid decellularized osteochondral explants were used in this assay. A full-thickness defect 5 mm in diameter and 3 mm in depth (down to the subchondral bone) was created in each decellularized osteochondral explant using a drill (the red dotted region). A partial-thickness defect was also created from the edge of the full-thickness defect to the edge of the explant using a scalpel (the green dotted region). The explants were rinsed with sterile saline to remove any debris. Approximately 300 PA-MCTs or H-MCTs per explant were added and covered with a mixed hydrogel composed of collagen and fibrin. The hydrogel was quickly polymerized with thrombin, and each explant was transferred to an incubator for further polymerization. After the hydrogel was fully solidified, medium was added and each explant was cultured at 37 °C with 5% CO_2 for 5 extra weeks. The medium was changed twice a week and at least triplicate samples were assayed for each group.

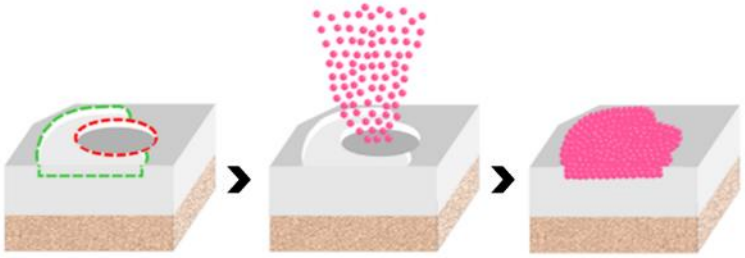

Figure S1. Illustration of the process of cartilage defect repair by the bio-assembly of PA-MCTs or H-MCTs in an osteochondral explant model. One corner of each explant was removed for ease of sample orientation during observation.

6.3. Large defect repair

6.3.1. Analysis the injectability of PA-MCTs

PA-MCTs of various sizes in a mixed hydrogel composed of collagen and fibrin were manually injected through glass tubes of various IDs using a syringe. The smallest ID of the glass tube tested was 1.4 mm, and the largest diameter of the PA-MCTs tested was ~650 μm. The injection process was monitored under an inverted microscope (Nikon). The injection of PA-MCTs to a cartilage defect in a sheep stifle joint was performed to mimic surgical implantation.

6.3.2. Injecting PA-MCTs to the defects

Irregularly-shaped (water-drop-like shape) large defects were created in decellularized sheep condyles using a curette. Each defect was made at least 11 mm in the long axis and down to the subchondral bone. Approximately 800 PA-MCTs were injected into each defect in a mixed hydrogel composed of collagen and fibrin. The injection device (~3.3 mm OD and ~2.5 mm ID, Figure S13, Supporting Information) was made by slicing off the proximal section of a repeat pipette tip (Eppendorf). After injection, the hydrogel was quickly polymerized with thrombin, and then each condyle was transferred to an incubator for further polymerization. After the hydrogel was fully solidified, medium was added, and samples were cultured for extra 5 weeks. At least triplicate samples were assayed.

7. Generating customized osteochondral allografts

De-identified computed tomography images of a human knee, which were stock in our lab, were imported to 3D Slicer software, and the 3D volumetric reconstruction was performed and exported as an STL file. [5] The STL file was further processed using Blender software [6] : (i) generating a cartilage layer from the bone surface, (ii) generating a cartilage defect in the weight-bearing region of the medial femoral condyle, (iii) mimicking the preparation process of the defect site, and (iv) designing an osteochondral allograft 1 cm in diameter. Decellularized bone plugs (curved top, 1 cm in diameter and 8 mm in height) were created using the same protocol as described above, matching the design of the plugs in the 3D model. Following the same protocol as described above: (i) bone plugs were placed into agarose wells; (ii) PA-MCTs were cultured for 2 weeks and then collected and placed onto the bone plugs together with a mixed hydrogel composed of collagen and fibrin; and (iii) the constructs were further cultured in the medium for 5 extra weeks and the fidelity was evaluated by two independent scientists.

8. Resurfacing an entire condyle by PA-MCT bio-assembly.

Femoral condyles were removed from the hind limbs of adult New Zealand White rabbits that were humanely euthanized. Cartilage and other soft tissues were removed from the condyles with a scalpel. The condyles then went through the decellularization process mentioned above and were sterilized with 70% ethanol and rinsed with PBS. To resurface a condyle, two layers of ~800 PA-MCTs after 2 weeks of culture, were manually applied to the bony surface together with a small volume of a mixed hydrogel composed of collagen and fibrin. The PA-MCTs attached to the bony surface without extra support. The constructs were cultured in the medium at 37 °C with 5% for 5 extra weeks.

9. Drug screening

As a proof of concept, we chose 4 drugs with known anti-inflammatory effects: dexamethasone (corticosteroid, Sigma-Aldrich), Celecoxib (non-steroidal anti-inflammatory, Pfizer), IGF-1 (growth factor, StemImmune) and TGF-β (growth factor, StemImmune). PA-MCTs were cultured for 2 weeks and then collected and added into wells of a 96-well plate. Then dexamethasone, Celecoxib, IGF-1, and TGF-β were added. One hour later, IL-1β (StemImmune) was added to each well. GAG content was analyzed by dimethyl methylene blue assay (DMMB) assay (details in section 15) after 3 days, and expression of cartilage-related genes (Table S5) was analyzed by qPCR after 5 days.

The ranking of cartilage positively related genes was based on the sum of gene expressions of Sox9, collagen type II and ACAN, where the rank score of the highest value is 4 and the lowest value is 1.

The ranking of inflammatory genes was based on the sum of gene expressions of MMP-3 and MMP-13, where the rank score of the lowest value is 4 and the highest value is 1. The

ranking of overall anti-inflammatory effects was evaluated by combining the ranking score over GAG contents, expression of inflammatory genes and cartilage positively related genes.

Table S2. Ranking of the disease-modifying effects of the drugs

Ranking Score	IL-1β+DEX	IL-1β+IGF-1	IL-1β+TGFβ	IL-1β+CEL
Cartilage-Positive-Genes	2	3	4	1
Anti Inflammation-Genes	4	3	2	1
GAG Content	4	3	2	1
Overall	10	9	8	3

DEX: Dexamethasone, CEL: Celecoxib

10. Microinjection

Grooves were generated in an agarose gel using a mold. PA-MCTs were aspirated and transferred into the grooves, and individual PA-MCTs were manually adjusted to be spread apart from each other. A pre-pulled glass pipette (WPI) was mounted on a micromanipulator and connected to a syringe pump. A solution of 10 μl of FITC-dextran was aspirated into the glass pipette. Under a stereo-microscope and using a micromanipulator, the tip of the glass pipette was inserted into one PA-MCT at a time, and the FITC-dextran was injected. Because a PA-MCT contains dense matrix and the pressure inside it is high, the volume of the injected solution was controlled by the pump execution time. The size of the yellow circle (bright field color of FITC-dextran solution) was also used as a secondary volume indicator. The success of injecting FITC-dextran was determined by fluorescence microscopy.

11. Cell viability assay

A calcein-AM (Invitrogen) staining assay was used to evaluate cell viability within the first 3 days post bioprinting. A CellTiter-Glo 3D Cell Viability (Promega) assay was used to analyze cell

viability from the 4th day post bioprinting, and data were normalized to DNA content, which was measured by a PicoGreen assay (Promega). All the assays were performed according to instructions from the manufacturers.

12. Macroscopic Imaging

Macroscopic images were taken under a stereo-microscope equipped with a 5MP digital camera (Motic). The magnification scale was calculated each time with a calibration slide placed at the same focal depth as the sample.

13. Histological Staining

13.1. Tissue harvest and process

Samples without bone tissues, namely individual PA-MCTs, H-MCTs and bio-assembled macro-tissues, were collected, rinsed with PBS, fixed with paraformaldehyde, dehydrated through a graded ethanol series, embedded in paraffin, and sectioned into slices of 5 μm thickness using a microtome (Microm).

After fixation, all other samples consisting of bone tissues were decalcified with formic acid and then were processed through the same procedures as above.

13.2. Safranin O and Alcian blue staining

Slides were deparaffinized with Xylene Substitute (Leica) and were rehydrated through a graded ethanol series. An Alcian blue solution (counterstained with fast red, Sigma-Aldrich) and a Safranin O solution (counterstained with fast green, Sigma-Aldrich) were used to stain sulfated glycosaminoglycans (sGAG). Both Alcian blue and Safranin O staining were performed for most of the samples.

13.3. GAG semi-quantification by image processing

Color intensities in a blue or red channel of slides stained with Alcian blue or Safranin O solutions have been reported to correlate with GAG content. [7] To determine linearity and the degree of correlation between dye concentrations (Alcian blue and Safranin O) and color intensities, stock dye solutions were diluted into a series of concentrations and pipetted into a 96-well plate. The solutions were imaged under a microscope through a 5-megapixel color camera. The identical condition was utilized for each image acquisition, including the illuminating light intensity (a LED light source was used to precisely control light illumination), objectives, exposure time, and white balance. Relative GAG content was quantified by calculating color intensities within the blue (Alcian blue) or red (Safranin O) channel of captured images respectively, using ImageJ. [3] With the coefficient of determination (R^2) being 0.9961, we found that the dye concentration highly correlates with the color intensity.

To analyze relative GAG content in tissue sections, slides were stained with Alcian blue and Safranin O solutions, imaged and analyzed using the identical protocol described above. Specifically, to study the mechanism of PA-MCT bio-assembly and to compare the GAG content inside and between PA-MCTs, pixel intensities along a series of parallel lines spanning inside and outside spaces of the PA-MCTs were analyzed (Figure S10A, B, Supporting Information). To evaluate the quantity of neocartilage inside articular cartilage defects and to analyze the distribution of GAG content throughout neocartilage inside the defects, 2D pixel intensity mapping was performed using ImageJ.

13.4. Immunohistochemistry

Slides were incubated in a citrate buffer solution in a microwave to retrieve antigens. Nonspecific binding was reduced by pre-incubating slides with a bovine serum albumin solution.

Slides were then incubated with an anti-collagen type II antibody (CIIC1, Developmental Studies Hybridoma Bank) at 4 °C overnight. They were further incubated with an Alexa Fluor 488-labeled anti-mouse secondary antibody (Bio legend) in 5% (w/v) bovine serum albumin (BSA) for 12 h at room temperature. Slides were then mounted and imaged under a fluorescence microscope (Nikon) equipped with a monochrome camera (SPOT Imaging). Similar to the semi-quantification of GAG content, the content of collagen type II was determined by analyzing the color intensities of the fluorescent images using ImageJ.

13.5. Whole-mount Alcian blue staining

Assembled macro-tissues were rinsed with PBS, fixed with paraformaldehyde and rinsed with PBS again. Each sample was then submerged in an Alcian blue solution for GAG staining and rinsed extensively to remove any unbound dye.

14. Scoring bioprinted individual PA-MCTs and H-MCTs and defect repair

Table S3. Modified Bern Score system for evaluating individual bioprinted PA-MCTs and H-MCTs [7] (Minimum Score: 0; Maximum Score: 9; Section: 5 μm thickness)

Scoring categories	Score
A. Uniformity and darkness of Safranin O–fast green staining and immunohistochemical staining for collagen type II	
No stain	0
Weak staining of poorly formed matrix	1
Moderately even staining	2
Even dark stain	3
B. Distance between cells/level of matrix accumulated	

High cell densities with no matrix in between (no spacing between cells)	0
High cell densities with a low amount of matrix in between (cells < 1 cell-size apart)	1
Moderate cell density with a medium amount of matrix (cells approx. 1 cell-size apart)	2
Low cell density with a moderate distance between cells (> 1 cell) and a high amount of matrix	3
C. Cell morphologies represented	
Condensed/necrotic/pycnotic bodies	0
Spindle/fibrous	1
Mixed spindle/fibrous with rounded chondrogenic morphology	2
Majority rounded/chondrogenic	3

Table S4. Modified O'Driscoll Score for evaluating osteochondral defects repair using PA-MCTs and H-MCTs [8] (Minimum Score: 0; Maximum Score: 22; Section 5 μm thick)

Characteristic	Grading	Score
1. Hyaline cartilage	80%–100%	8
	60%–80%	6
	40%–60%	4
	20%–40%	2
	0%–20%	0

2. Structural characteristics		
A. Surface regularity	Smooth and intact	2
	Fissures	1
	Severe disruption, fibrillation	0
B. Structural integrity	Normal	2
	Slight disruption, including cysts	1
	Severe lack of integration	0
C. Thickness	100% of normal adjacent cartilage	2
	50–100% of or thicker than normal	1
	0–50% of normal	0
D. Bonding to the adjacent cartilage	Bonded at both ends of the graft	2
	Bonded at one end, or partially at both ends	1
	Not bonded	0
3. Freedom from cellular changes of degeneration	Normal cellularity, no clusters	2
	Slight hypocellularity, < 25% cluster	1
	Moderate hypocellularity, > 25% cluster	0
4. Bonding of repair cartilage to native subchondral bone	complete and uninterrupted	2
	< 100% but > 50% reconstitution	1
	< 50% complete	0
5. Safranin O staining of the matrix	> 80% homogenous positive stain	2
	40%–81% homogenous positive stain	1

< 40% homogenous positive stain	0

15. DMMB assay

A dimethyl methylene blue assay (DMMB) was used to determine the content of GAG in PA-MCTs and H-MCTs.[9] In brief, PA-MCTs, H-MCTs, assembled macro-tissues and native articular cartilage were collected, rinsed with PBS and digested with papain. The digested solution was reacted with DMMB (Sigma-Aldrich), and absorbance was measured at 492 nm. Using the absorbance of standard chondroitin sulfate (Sigma-Aldrich) as a standard curve, GAG content in the samples was calculated accordingly.

To compare the homogeneity between native articular cartilage explants and PA-MCTs, explants—at a typical size of 3 mm in diameter and 1 mm in height—were harvested from the medial femoral condyle, lateral femoral condyle, medial tibial plateau and lateral tibial plateau (triplicate samples were harvested from each location). Relative GAG content in the explants and PA-MCTs was analyzed using the DMMB assay described above. The coefficient of variation of the GAG content of PA-MCTs was calculated using DMMB-readouts of at least 5 randomly selected samples. The coefficient of variations of the GAG content of native cartilage explants was calculated using DMMB-readouts of samples from each region or the entire knee.

16. Quantitative real-time PCR

To examine the specific gene expression listed in Table S5, samples were collected and rinsed with PBS. Total RNAs in PA-MCTs and H-MCTs were extracted using an RNeasy Mini Kit (Qiagen) according to the manufacturer's instruction. Samples were treated with DNase I removing any possible genomic DNA contamination. Concentrations and purities of the RNA samples were determined by a NanoDrop 2000 spectrophotometer (Thermo scientific). Total RNAs were reverse-transcribed into cDNAs using a SuperScript III kit (Invitrogen) following the

manufacturer's instruction. Real-time PCR was performed using a SYBR Green PCR Master Mix (Applied Biosystems) in a thermal cycler. Gene expression of collagen type II (COL2A1), collagen type I (COL1A1), aggrecan (ACAN), Sox 9, MMP-3 and MMP-13 was analyzed. The primer sequences are listed in Table S5. Articular cartilage tissues from the same bovine source were used as a positive control in the PCR reaction. mRNA expression levels of the target genes were normalized to that of the 18S rRNA reference gene. Relative expression of the genes of interest was quantified using a ΔΔCT method.

Table S5. Forward and reverse primers used qRT-PCR analysis

Species	Gene Name	Primer Sequence (5'–3')
Bovine	COL2A1	Forward CCA CTG CAA GAA CAG CAT TG
		Reverse CCA GTT CAG GTC TCT TAG AG
	COL1A1	Forward CAG CCG CTT CAC CTA CAG C
		Reverse TTT TGT ATT CAA TCA CTG TCT TGC C
	ACAN	Forward CAC TGT TAC CGC CAC TTC CC
		Reverse GAC ATC GTT CCA CTC GCC CT
	Sox9	Forward CAT GAA GAT GAC CGA CGA G
		Reverse GT CTT CTC CGT GTC GGA
	MMP-3	Forward TTA GAG AAC ATG GGG ACT TTT TG
		Reverse CGG GTT CGG GAG GCA CAG
	MMP-13	Forward ATT CTT CTG GCG GCT GCA TCC
		Reverse AGG CGG CAT CAA TAC GGT TGG
Human	COL2A1	Forward GGA CTT TTC TTC CCT CTC T
		Reverse GAC CCG AAG GGT CTT ACA GGA

	COL1A1	Forward CAGCGTCACTGTCGATGGC
		Reverse AACGTCGAAGCCGAATTCC
	ACAN	Forward CATTCACCAGTGAGGACCTCGT
		Reverse TCACACTGCTCATAGCCTGCTTC
	Sox9	Forward AAC GCC GAG CTC AGC AAG A
		Reverse CCG CGG CTG GTA CTT GTA ATC
Bovine & Human	18S rRNA	Forward AAA CGG CTA CCA CAT CCA AG
		Reverse CCT CCA ATG GAT CCT CGT TA

qRT-PCR, quantitative reverse transcription-polymerase chain reaction; COL2A1, collagen type II; COL1A1, collagen type I; ACAN, aggrecan; Sox9, SRY-Box transcription factor 9; MMP-3, matrix metalloproteinase-3; MMP-13, matrix metalloproteinase-13

17. Mechanical Tests

17.1 Micropipette Aspiration

A micropipette aspiration technique was used to measure the stiffness of individual PA-MCTs or H-MCTs using a protocol reported previously with some modification. [10] In short, as shown in Figure S2 below, 2/3 of a glass micropipette was mounted horizontally inside a Petri dish placed on an inverted microscope stage (Nikon), while the remaining 1/3 was extruded outside the Petri dish via a drilled hole through the wall of the dish. The end inside the Petri dish was open, and the other end was connected to a negative pressure source through Tygon tubing. Pressure differences between the two ends of the micropipette (ΔP) were recorded via a digital pressure meter. To measure the hardness of PA-MCTs or H-MCTs, one PA-MCT or H-MCT at a time was placed at the open end of the micropipette under a workstation magnifier. Monitored from the inverted microscope, the PA-MCT or H-MCT was aspirated and quickly sealed the open end of the glass micropipette when an initial ~1 kPa negative pressure was applied. The pressure

was then changed at a constant speed of 2 kPa/step, and an image was captured per step of pressure change. The inner radius of the glass micropipette was denoted as Ri; the length of the tongue inside the pipette was denoted as X, and the initial X was denoted as X_0. The current assay was terminated when -90 kPa pressure was reached or when $X > R_i$. Pressure differential (ΔP) versus normalized deformation $(X - X_0)/R_i$ was plotted, and stiffness values of PA-MCTs and H-MCTs were calculated by curve fitting.

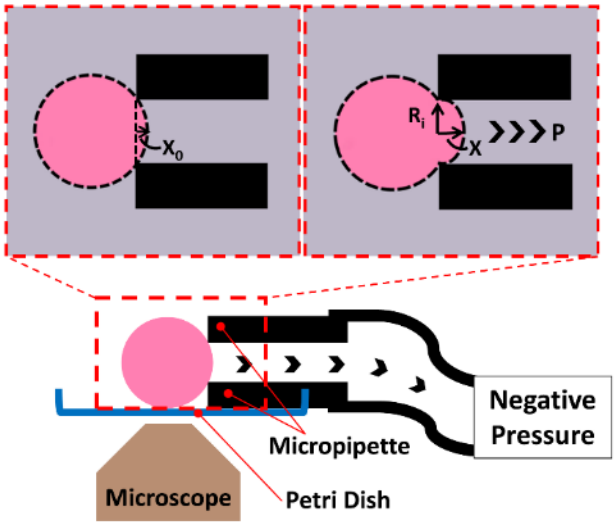

Figure S2. Illustration of the micropipette aspiration assay.

17.2. Confined and unconfined compression tests

In a confined compression test (Figures S3C, D), specimens were placed in a PBS bathed testing chamber inside a universal testing machine which is comprised of a ball-screw guide rail driven by a servo motor (Panasonic) and a displacement encoder with the resolution of 0.5 µm (Panasonic) and load cells (HBM). The chamber base is made of impermeable stainless steel with a center circular well. Samples were punched into disks to match the inner diameter of the well for a tight contact when placed into the well. The cartilage surface was compressed with a stainless-steel porous indenter at a speed of 1 µm s^{-1} until a 20% strain was reached. The sample was allowed for stress relaxation to equilibrium that was determined when the change of stress

was less than 0.003 MPa over 180 s or when the relaxation was over 3600 s. Aggregate modulus H_A and Permeability k_0 were then calculated using a biphasic model. [11]

An unconfined compression test (Figures S3A, B) was used to determine Young's Modulus using the identical set-up to the confined compression test except specimens were compressed between two non-permeable platens.

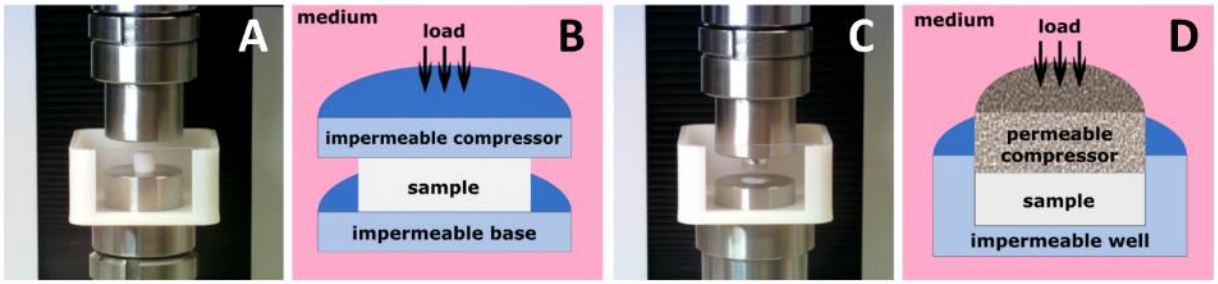

Figure S3. Photographs of the device (A, C) and schematics of the mechanical tests (B, D). Samples were tested using unconfined (A, B) and confined (C, D) compression tests in a testing chamber supplemented with a saline solution (A, C), which was omitted while being photographed.

17.3. Push-out test

As shown in Figure S4 below, upon completing a defect repairing assay, cartilage proportions were sliced off the constructs (A), and the height of each removed cartilage was measured (B). The removed cartilage tissues were, one tissue at a time, placed into a specimen holder (C) and transferred to the universal testing machine (D) that was described above (section 17.2). To test the adhesion force between each neocartilage and the surrounding native cartilage, a rigid 4 mm diameter indenter was moved down to push the center of the specimen at 1μm s^{-1} until a tissue separation occurred. The maximum force was normalized by the lateral area of the interface between the neocartilage and native cartilage. Each resulting value was recorded as the failure stress.

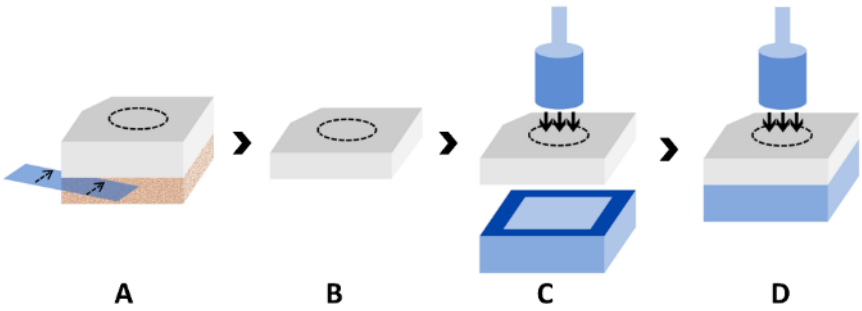

Figure S4. Illustration of the push-out assay.

18. Statistical analysis

Data were statistically analyzed using JASP (University of Amsterdam). As appropriate, one-way ANOVA in conjunction with Tukey post hoc analysis was used to determine differences among groups, and the independent-samples t test was used to determine differences between two groups. Levene's test was used to determine differences of the coefficient of variations among groups. A *P*-value below 0.05 was considered to be significantly different.

References:

[1] Y. Pang, B. Grottkau, *Three dimensional microtissue bioprinter*, **2017**.

[2] B. E. Grottkau, Z. Hui, Y. Pang, *International Journal of Molecular Sciences* **2020**, *21*, 3482.

[3] C. A. Schneider, W. S. Rasband, K. W. Eliceiri, *Nat. Methods* **2012**, *9*, 671.

[4] Y. Pang, A. A. Ucuzian, A. Matsumura, E. M. Brey, A. A. Gassman, V. A. Husak, H. P. Greisler, *Biomaterials* **2009**, *30*, 2023.

[5] R. Kikinis, S. D. Pieper, K. G. Vosburgh, In *Intraoperative Imaging and Image-Guided Therapy* (Ed.: Jolesz, F. A.), Springer, New York, NY, **2014**, pp. 277–289.

[6] B. Foundation, *blender.org*.

[7] K. S. Deoras, M. R. Wolfson, R. L. Searls, S. R. Hilfer, T. H. Shaffer, 6.

[8] A. Getgood, F. Henson, C. Skelton, E. Herrera, R. Brooks, L. Fortier, N. Rushton, *Cartilage* **2012**, *3*, 351.

[9] R. Farndale, D. Buttle, A. Barrett, *Biochimica et Biophysica Acta (BBA) - General Subjects* **1986**, *883*, 173.

[10] R. M. Kleinberger, N. A. D. Burke, K. Dalnoki-Veress, H. D. H. Stöver, *Materials Science and Engineering: C* **2013**, *33*, 4295.

[11] W. M. Lai, V. C. Mow, *BIR* **1980**, *17*, 111.

Supplementary Results

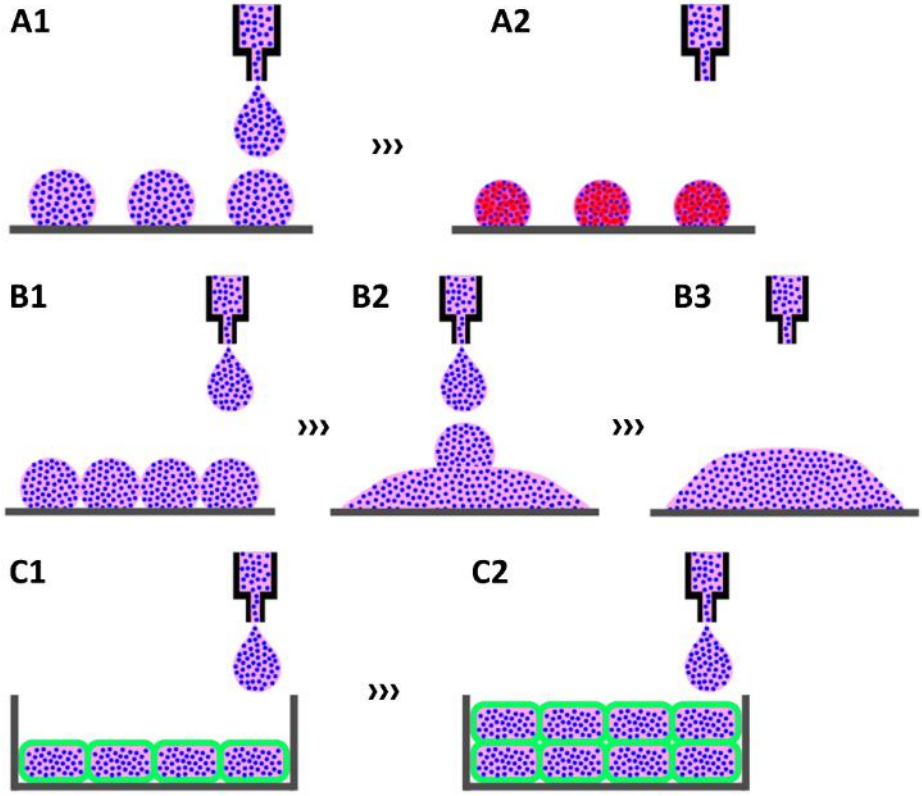

Figure S5. Illustration of limitations of existing DOD bioprinting technologies. When droplets of bioink are deposited onto a substrate discretely, the diameter of each droplet can be controlled to be less than 100 μm (A1). However, being so small, a droplet may evaporate quickly, and this dramatically impairs cell viability making this approach impractical (A2). Therefore, multiple to a large number of droplets are required to be deposited adjacent to each other to counteract evaporation. However, once a droplet contacts with its neighbor droplets (B1), they merge together in the first layer and in any layers above (B2). Eventually, a construct with a global homogeneous cell distribution forms (B3) thus it is not possible to pattern cells into clusters inside a bioprinted construct at a micro-scale. Another approach is to quickly polymerize a droplet upon deposition to the substrate (C1) or an existing layer (C2) to form one cell cluster per droplet. However, hydrogel interfaces (shown as green lines) are generated between any neighboring droplets. This limits the

interaction of cells between different droplets and limits tissue remodeling as well as impairs tissue maturation. In summary, none of the existing DOD bioprinting technologies can be used to practically and usefully pattern cells into clusters as a biophysical signal. Pink: hydrogel, blue dots: cells.

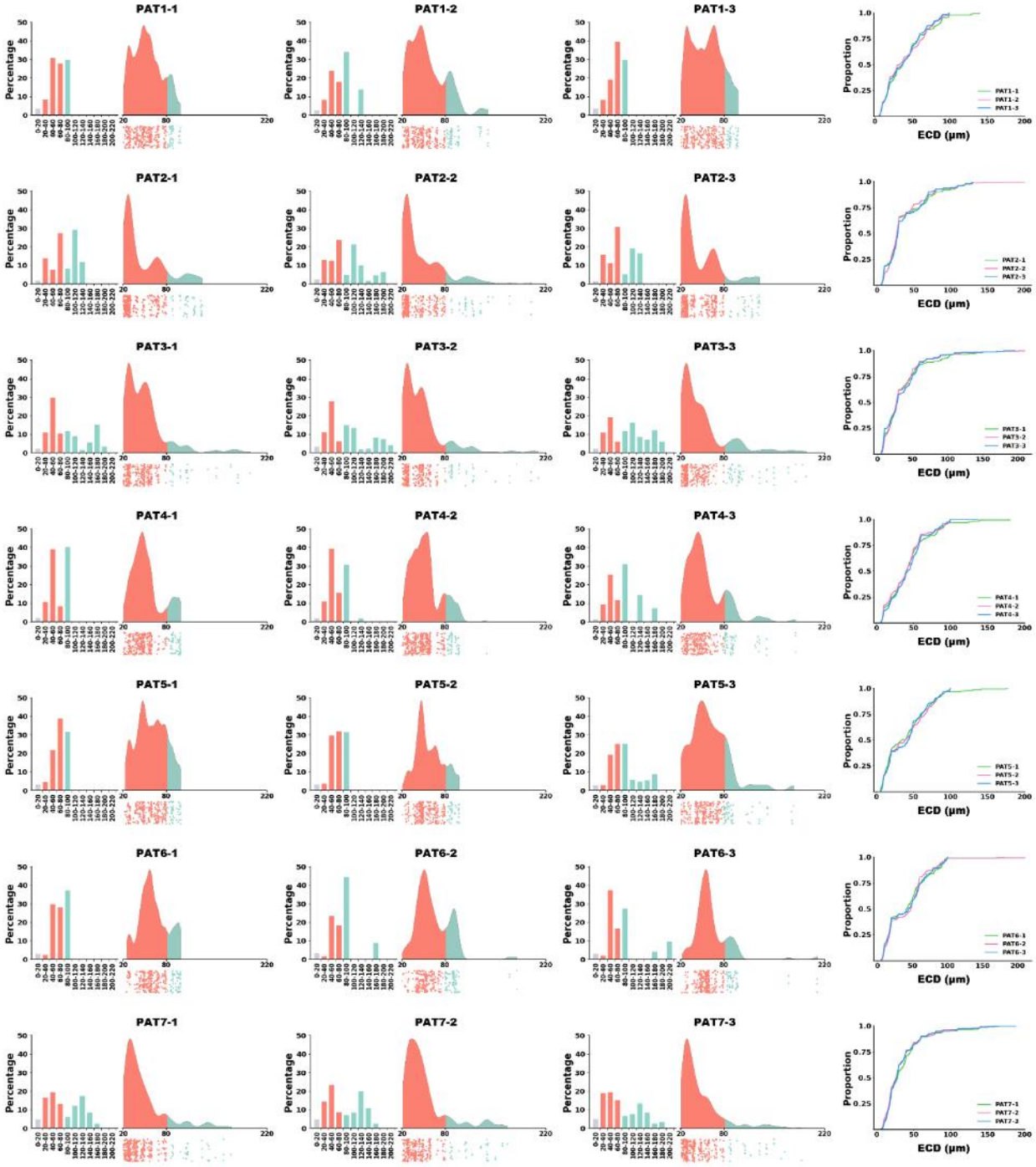
PAT1-1
PAT1-2
PAT1-3
PAT2-1
PAT2-2
PAT2-3
PAT3-1
PAT3-2
PAT3-3
PAT4-1
PAT4-2
PAT4-3
PAT5-1
PAT5-2
PAT5-3
PAT6-1
PAT6-2
PAT6-3
PAT7-1
PAT7-2
PAT7-3
Percentage
Proportion
ECD (μm)

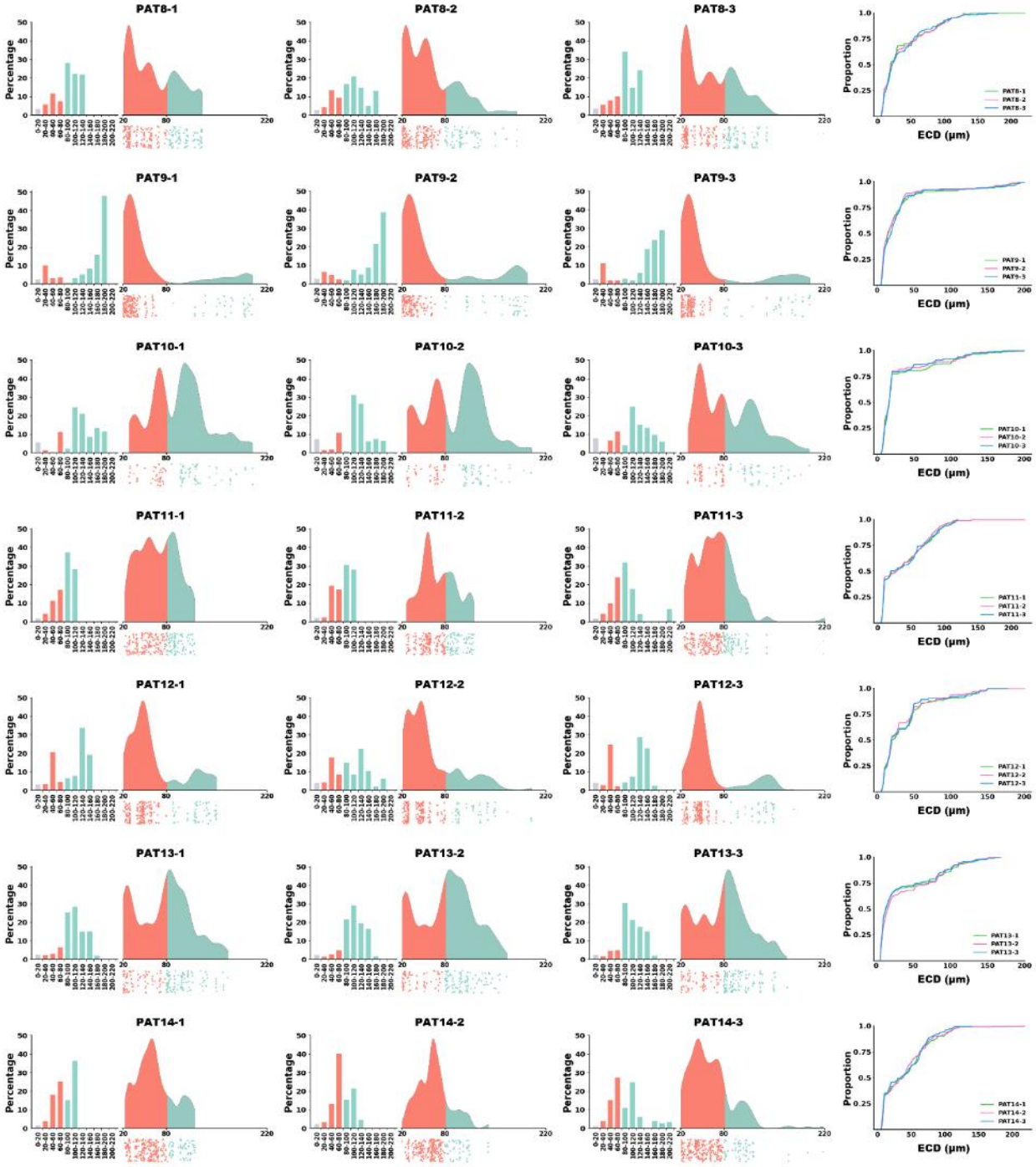
PAT8-1
PAT8-2
PAT8-3
PAT9-1
PAT9-2
PAT9-3
PAT10-1
PAT10-2
PAT10-3
PAT11-1
PAT11-2
PAT11-3
PAT12-1
PAT12-2
PAT12-3
PAT13-1
PAT13-2
PAT13-3
PAT14-1
PAT14-2
PAT14-3
Percentage
Proportion
ECD (μm)

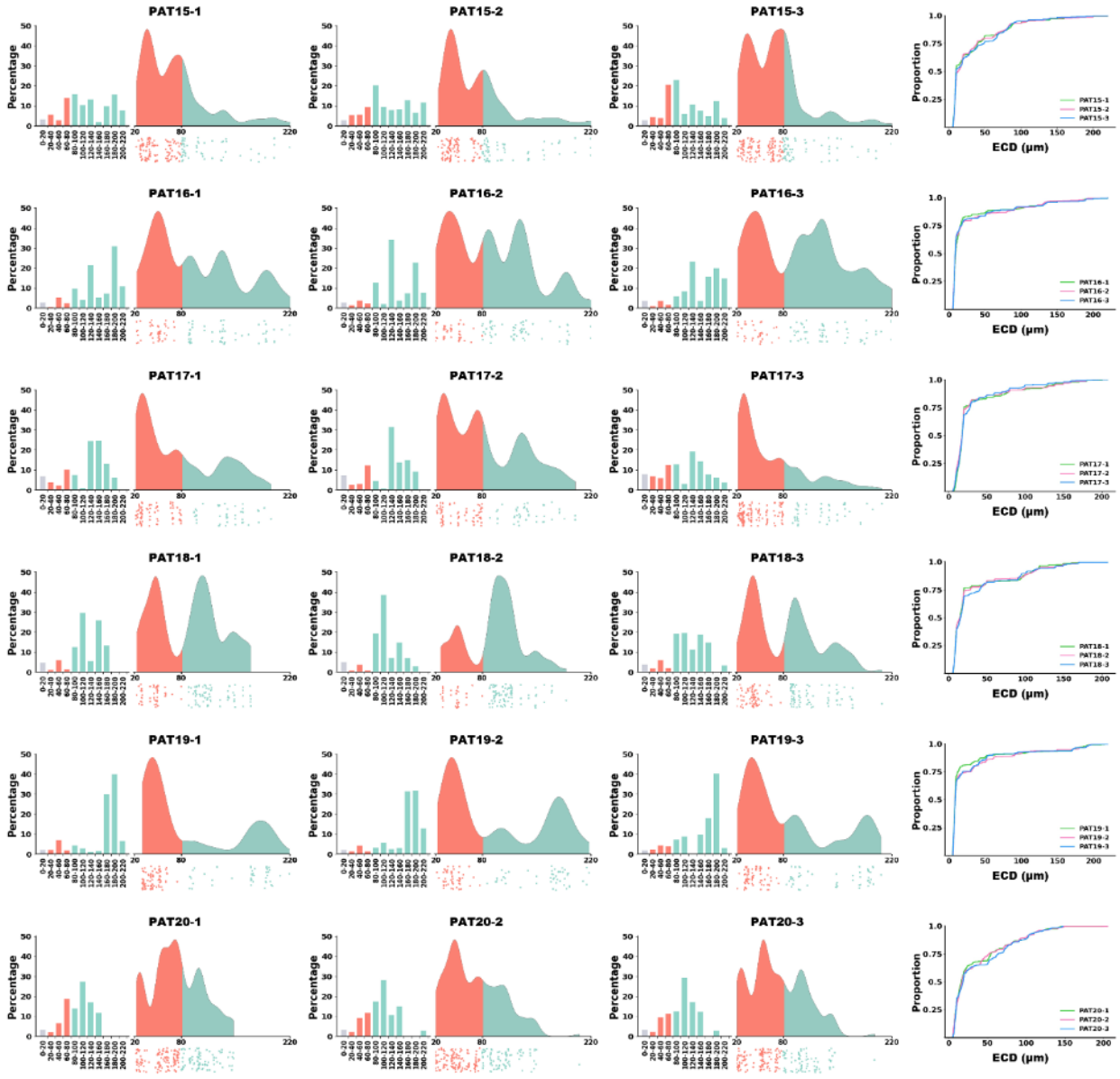

Figure S6. The area percentage bar plots, raincloud plots and ECDF plots of 20 unique patterns (three replicates of each pattern). ECD ranges between 20 and 80 μm, the selected optimized range, are shown in red.

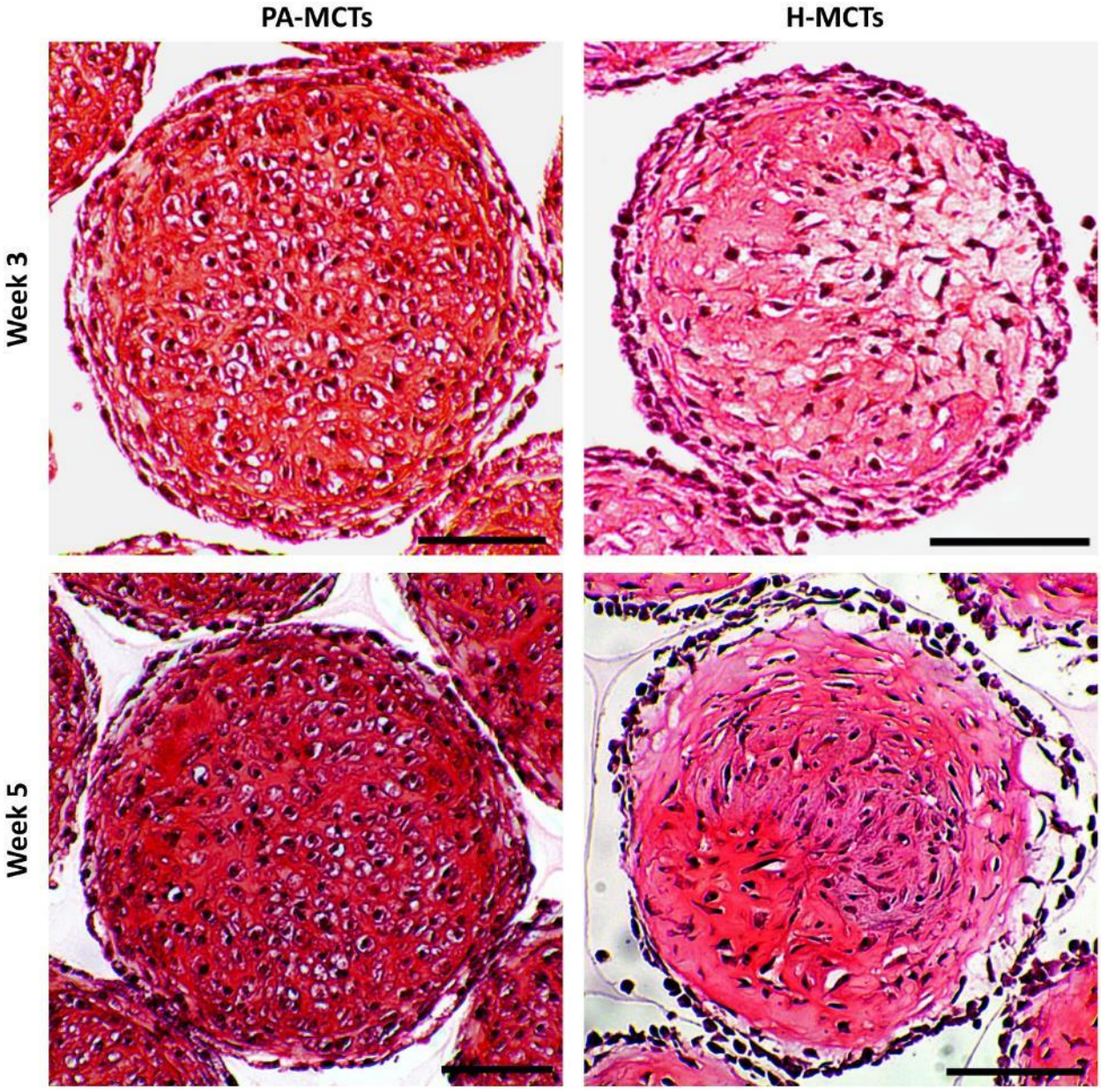

Figure S7. High-resolution representative images of typical Safranin O staining of PA-MCTs and H-MCTs. Scale bars = 100 μm. Same images at lower resolution are shown in Figure 4C.

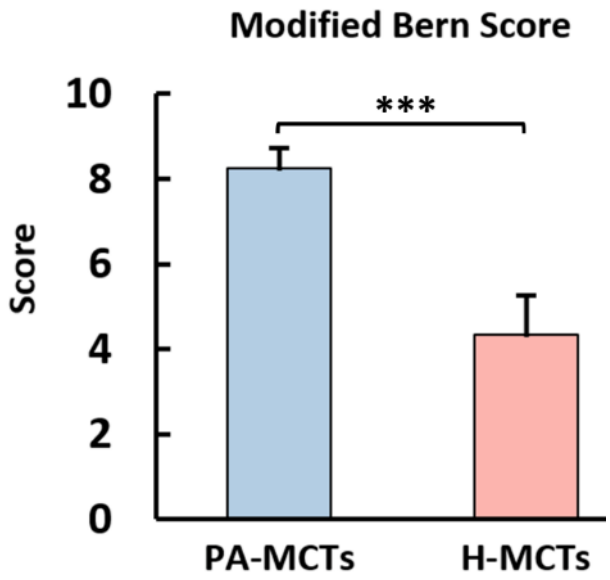

Figure S8. PA-MCTs demonstrate significantly higher Modified Bern Score than H-MCTs. n ≥ 3, data are means ± SD, *** $P < 0.001$ vs. H-MCTs by independent-samples t test.

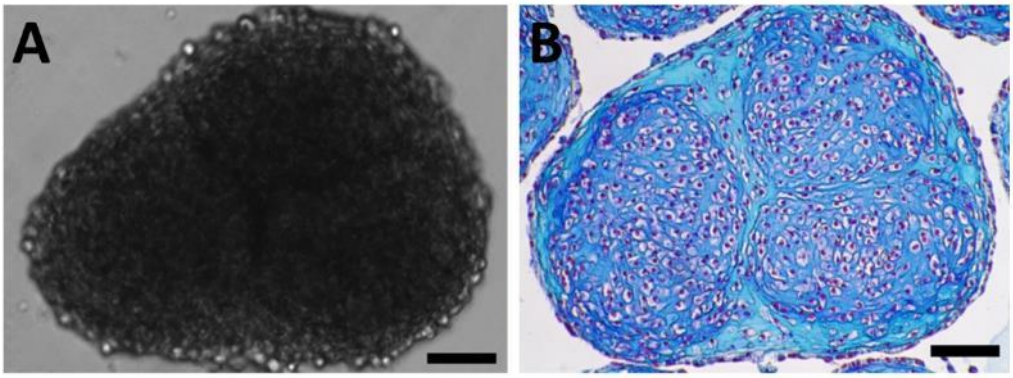

Figure S9. Demonstration of the early stage of PA-MCTs assembly (A: a phase-contrast image; B: a section stained with Alcian blue). PA-MCTs were cultured for 2 weeks and then collected and assembled. The images represent the status of week 4 of the total culture period. The blue color intensity of Alcain blue staining is linear to GAG content. Chondrocytes migrated from the insides of individual PA-MCTs into spaces between them where, as indicated by lighter blue, the GAG deposited by the migrated chondrocytes was relatively low at the early stage. Scale bars = 100 μm.

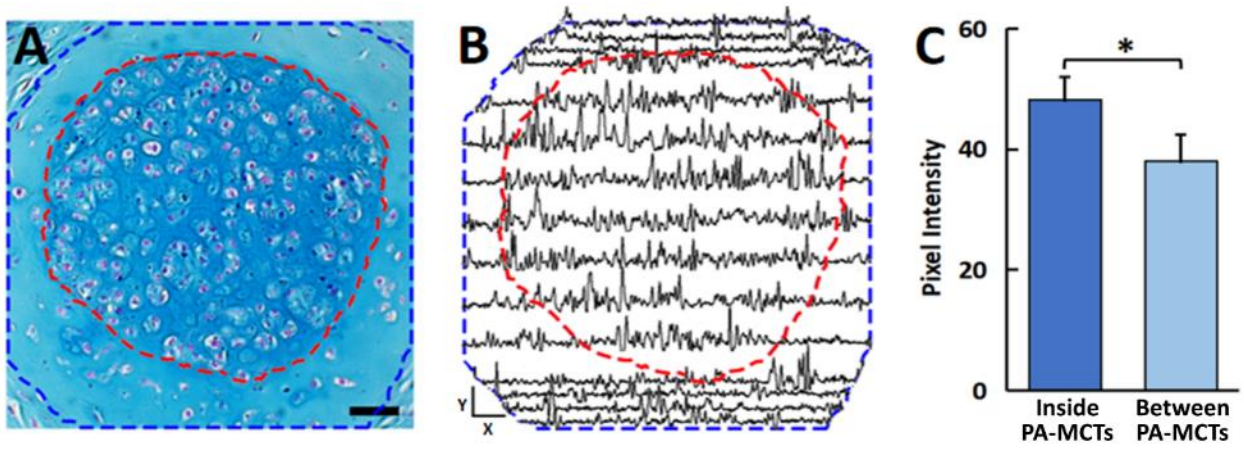

Figure S10. Semi-quantification of GAG content inside and outside PA-MCTs during cartilagenesis of bio-assembly. (A) A representative image of Alcian blue staining of a PA-MCT and the matrix around it at week 3 of the total culture period. Red and blue dashed regions indicate areas inside and outside the PA-MCT. Scale bar = 50 μm. The image is also shown in Figure 5C. (B) GAG content curves. Pixel intensities, representing relative GAG content, along a series of parallel lines across the image were analyzed. The height of each curve represents the level of GAG content. Y: Pixel intensity value, bar = 100; X: Distance, bar = 100 pixels. (C) Average GAG content inside PA-MCTs is significantly higher than outside PA-MCTs. $n \geq 3$, data are means ± SD, * $P < 0.05$ by independent-samples t test.

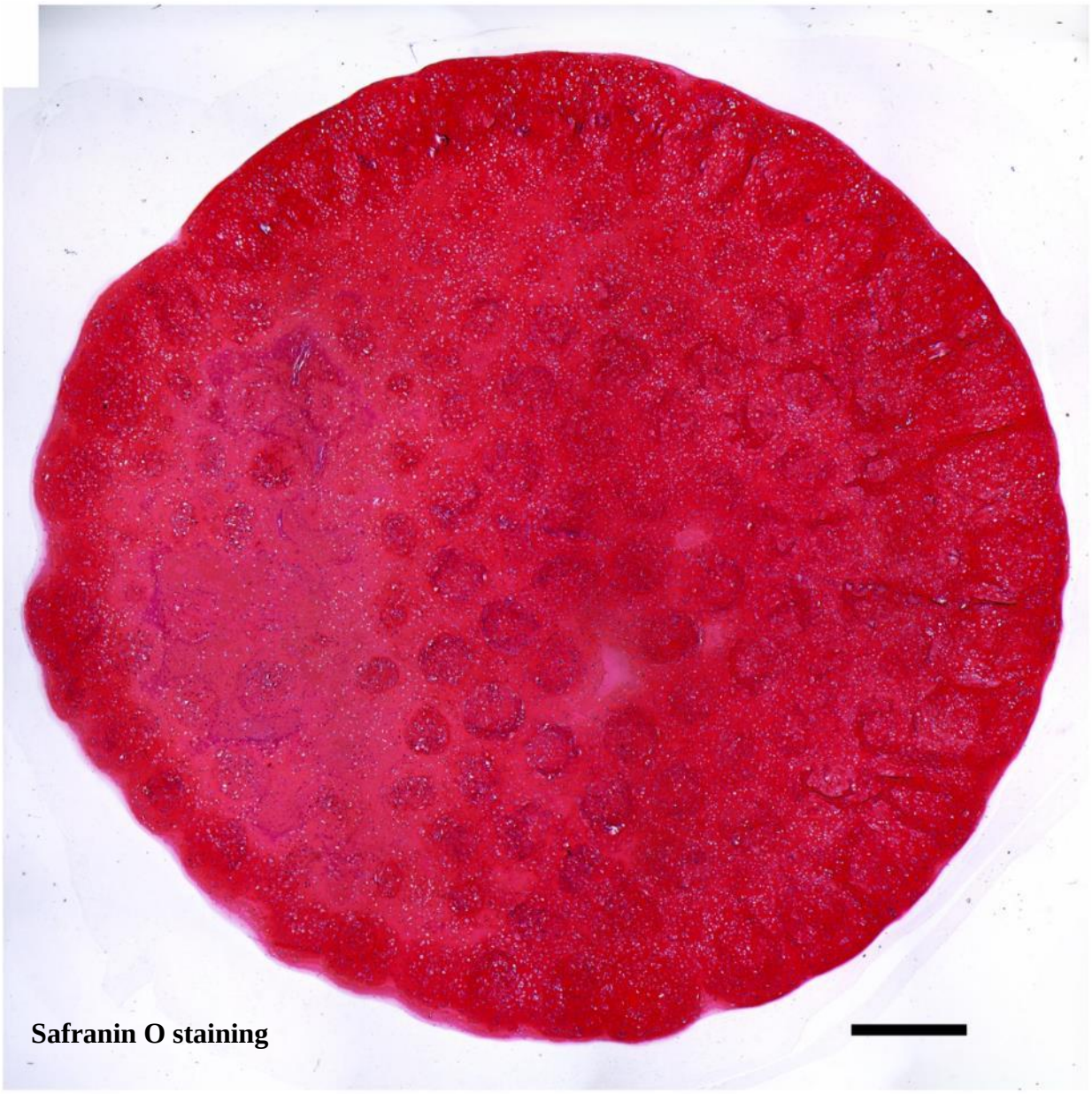

Figure S11. A representative histological image in high-resolution of an assembled macro-articular-cartilage tissue (week 7 of the total culture period, a panoramic view). PA-MCTs demonstrate the capability of cartilagenesis during the assembly process. Seamless histological assembly and extensive GAG expression throughout were visualized. Scale bar = 1 mm. The same image at a lower resolution is shown in Figure 5F.

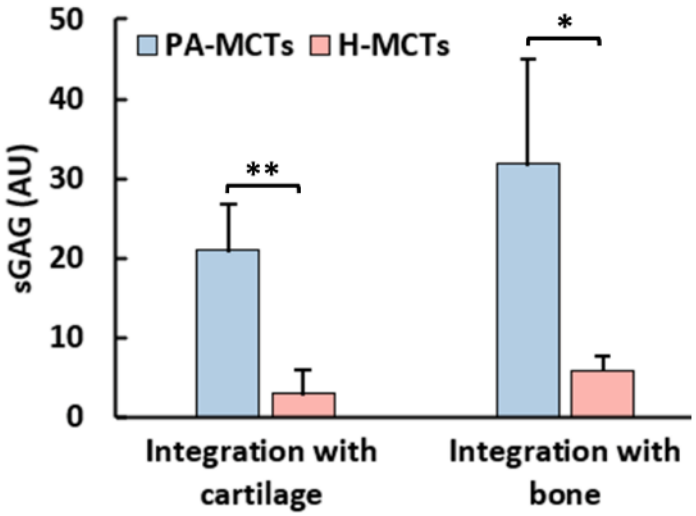

Figure S12. sGAG expression in the integration assay at week 7 of the total culture period. PA-MCT-assemblies demonstrated significantly higher GAG content than H-MCTs-assemblies evaluated by semi-GAG-quantification. n ≥ 3, data are means ± SD, * $P < 0.05$, ** $P < 0.01$ vs. H-MCTs by independent-samples t test.

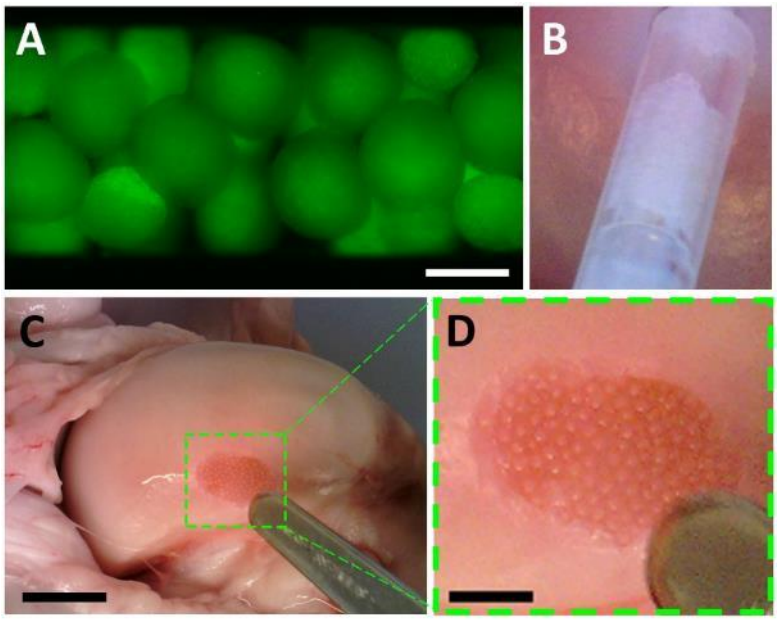

Figure S13. Demonstration of the delivery of PA-MCTs through injection. PA-MCTs with an average diameter of ~≤ 650 μm can be manually injected through a rigid tube as small as 1.4 mm ID smoothly by applying low pressure on the plunger. Figure A shows a microscopic image of PA-MCTs inside the glass tubing with a 1.4 mm ID. Figure B shows the injection device (~2.5 mm ID and ~3.3 mm OD) used for delivering PA-MCTs to the cartilage defects. The device's OD is smaller than the OD (4 mm) of a typical arthroscope. Therefore, the device can be suitable to be inserted into the human knee to inject PA-MCTs to the defect in a potential minimally invasive surgery. Figures C and D show the completion of injecting ~230 PA-MCTs to a defect created in a femoral condyle of a sheep knee. Scale bars = 500 μm (A), 1 cm (C), 3mm (D).

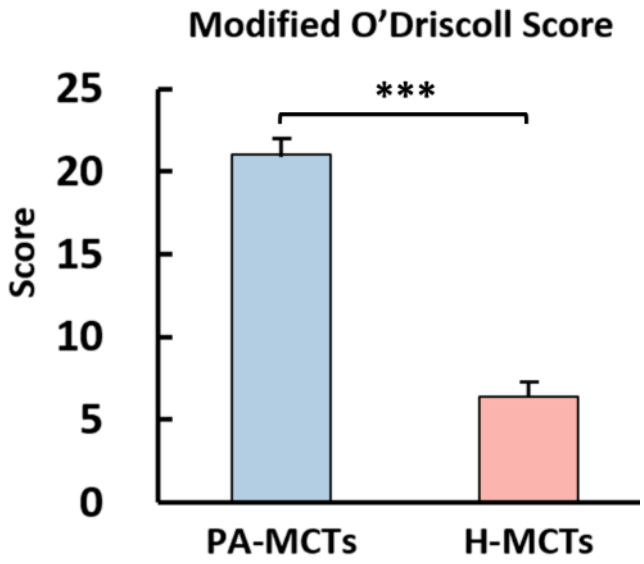

Figure S14. PA-MCTs demonstrated significantly higher Modified O'Driscoll Scores than H-MCTs in repairing osteochondral defects (week 7 of the total culture period). $n \geq 3$, data are means ± SD, *** $P < 0.001$ vs. H-MCTs by independent-samples t test.

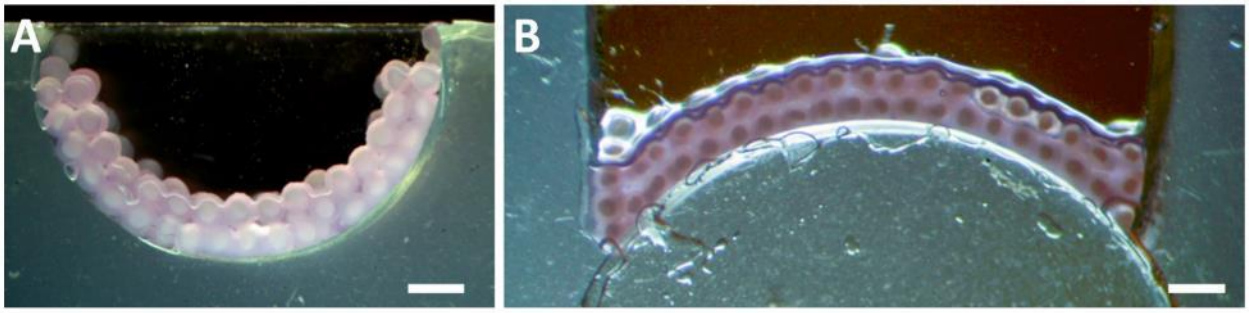

Figure S15. Demonstration of the capability of PA-MCTs for self-fitting curved surfaces. To evaluate the capability of PA-MCTs self-fitting curved surfaces of an articular joint for potential clinical implantation, silicone sheets with curved edges were used to mimic joint curves. Silicone sheets with convex (A) or concave (B) edges were placed between two glass slides. PA-MCTs were gently placed over each surface, and PA-MCTs self-fitted each curvature and attached to each surface seamlessly. Scale bars = 1 mm.

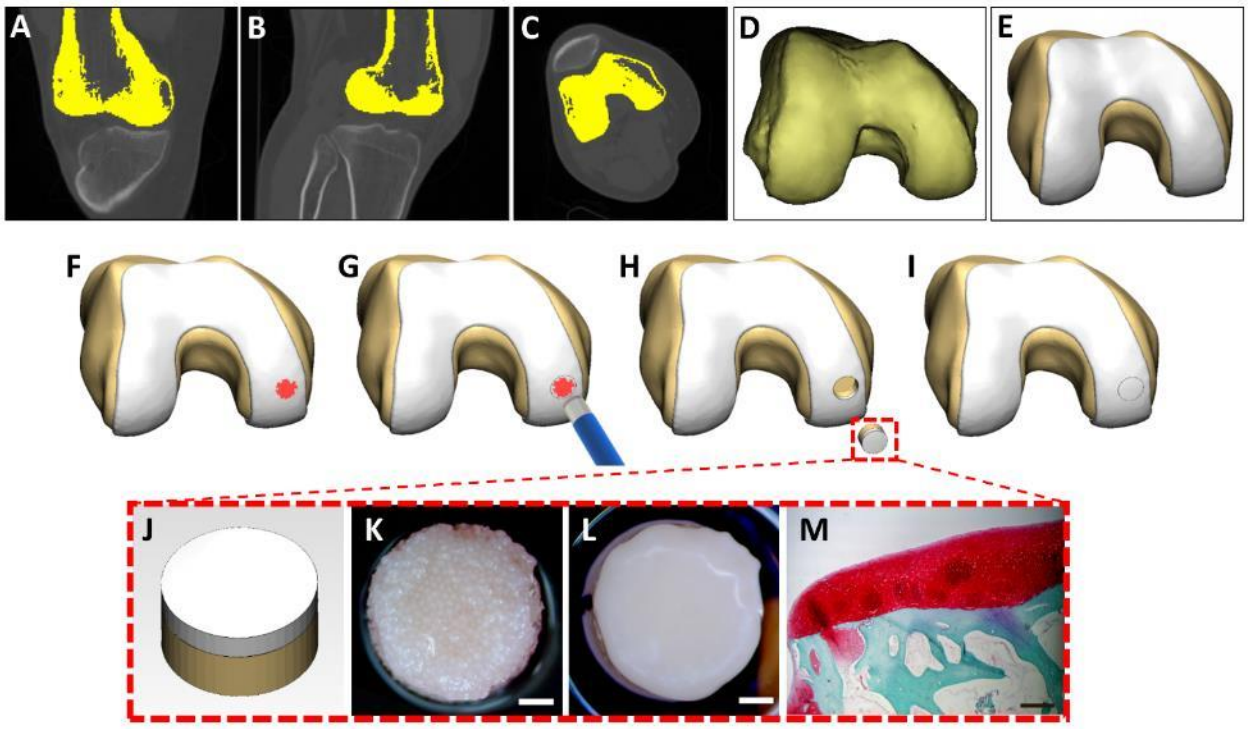

Figure S16. Generating personalized osteochondral allografts. Implantation of an osteochondral rather than cartilage-only allograft is necessary for cartilage defect diseases accompanied by an underlying bone lesion, such as osteochondritis dissecans. Natural allografts have the drawbacks of not fitting the geometry of a host knee and are of limited availability. To meet the clinical demand and provide a potential solution for osteochondritis dissecans lesions, here we present a proof-of-concept methodology generating personalized allografts using PA-MCTs and decellularized bone tissues. Engineered allografts were designed to fit the patient's dimensional information of the mimicked diseased knee joint in the following 4 steps. (i) Generating a healthy osteochondral model of a distal femur (A–E): regions of the femur bone were segmented from computed tomography images of a human joint (A–C); the distal femur bone was volumetrically 3D reconstructed (D); and a cartilage layer was created from the bone surface (E). (ii) Cartilage defect creation and allograft design (F–I): a defect was created on the weight-bearing region of the medial condyle (F, shown in red), and chondral lesion preparation was mimicked in the model (G). An

osteochondral allograft was designed to fit the defect (H, dashed line region; J, magnified view) and implantation was also mimicked (I). (iii) Generating an osteochondral allograft: according to the dimensional Information of the model (J), a cylindrical bone with a curved top was created and decellularized. Approximately 700 PA-MCTs were placed on top of the bone, where individual PA-MCTs were visible at week 1 (K). At week 7 of the total culture period, an osteochondral allograft (L) was generated with high shape and structural fidelity, matching the dimensional Information of the patient knee (J). The generated allograft has a smooth and white articular surface. Safranin O staining shows intense GAG expression and typical articular cartilage morphology in the cartilage layer of the allograft (M). Scale bars = 2 mm (K, L), 500 μm (M).